Electroactive biochar outperforms highly conductive carbon materials for biodegrading pollutants by enhancing microbial extracellular electron transfer

Amanda Prado,[1,2] Raúl Berenguer,[2,3,*] Abraham Esteve-Núñez[1,2,*]

[1] *Chemical Engineering Department, Universidad de Alcalá, Alcalá de Henares, Spain.*

[2] *Bioelectrogenesis Group, IMDEA Agua, Parque Tecnológico de la Universidad de Alcalá, 28805, Alcalá de Henares, Spain.*

[3] *Instituto Universitario de Materiales, Departamento Química Física, Universidad de Alicante (UA), Apartado 99, 03080 Alicante, Spain.*

Abstract

The development and full-scale application of microbial electrochemical technologies (METs) for wastewater treatment demand massive amounts of electroconductive carbon materials to promote extracellular electron transfer (EET) and biodegradation. While the potential capability of these materials and their properties to design efficient systems is still in their infancy, the state-of-the-art METs are based on highly-conductive fossil-derived carbons. In this work we evaluate the performance of different electroconductive carbon materials (graphite, coke, biochar) for supporting microbial EET and treating urban wastewater. Our results reveal that the electroconductive biochar was the most efficient biofilter-material, enabling to stimulate bioremediation at anodic potential as high as 0.6 V (maximum removal efficiency (92%) and degradation rate (185 g-COD $m^{-3}d^{-1}$)), and to fulfill the discharge limits under conditions where the other materials failed. A deep materials characterization suggests that, despite electroconductivity is necessary, the optimal EET on biochar can be mainly assigned to its large number of electroactive surface oxygen functionalities, which can reversibly exchange electrons through the geobattery mechanism. We propose the modulation of quinone-like e-acceptors by anodic polarization to promote the biodegradation capability of carbon materials. Because of its great efficiency and sustainability, electroactive biochar will greatly expand the applicability of METs at large scale.

* Corresponding authors:
email: abraham.esteve@uah.es
Tel: +34-918854950
email: raul.berenguer@ua.es
Tel: +34-965902364

1. Introduction

Microbial Electrochemical Technologies (METs) [1,2] constitute a plethora of emerging technologies based in the fascinating capacity of some microorganisms, so-called electroactive, for establishing a direct redox interaction with electrically conductive materials. Electrons produced by the metabolism of electroactive bacteria can be transferred to an electrode, which acts as terminal electron acceptor as any other natural acceptor like oxygen, nitrate or Fe(III)-oxides [3,4]. The clear advantage of exploiting electro-stimulated communities is that electrodes can boost microbial metabolism in anaerobic systems that are typically electron acceptor limited. Electroconductive material may represent an inexhaustible source of electron acceptors, hosting the additional advantage of providing a more easily modulated redox potential compared to standard, low-reducing redox species that generally drive these systems [5]. The redox potential of the electrode depends on the chemistry and bioelectrochemistry around the electrode. Moreover, the electrochemical characteristics of those microbial-assisted devices can be simply controlled by altering their configuration. Thus, they can be operated in different configurations, such as i) short-circuit Cell, with no resistors between electrodes [5-8]; ii) Microbial Electrochemical Cell (MFC), able to harvest energy in the presence of a resistor [1,2]; and iii) Microbial Electrolysis Cell (MEC) by poising a certain electrode potential through a potentiostat or a power source [1,2]. Regardless the configuration, one of the main application of MET is the wastewater treatment, a process based on oxidizing organic and inorganic matter coupled to a harvested microbial electrical current [1,2].

In spite of the limiting number of MET-based technologies with potential to reach full scale applications, there is at least one proved to be successful. Such application was originally inspired by the biofilter concept in constructed wetlands, a natural system for treating wastewater using inert material [9]. The integration of METs in the concept of a constructed wetland resulted in the so-called METland®, a new hybrid technology for treating urban wastewater in decentralized systems in a sustainable way with no energy cost [10]. The newborn configuration [5] was reported for the first time by constructing subsurface flow biofilters made of electroconductive coke able to clean-up urban effluents at rates higher that standard biofilters made of inert materials, like gravel. Such an enhancement was exclusively attributed to a positive effect of the electroconductivity of coke without any evidence of clogging classically associated to biofilter systems [5].

In this context, full scale applications of METland® using large carbon biofilters (> 50 m^3), are under construction at present [10]. The nature and properties of the carbon material may determine not only the performance of the biofilter, but also the cost and sustainability of this technology. However, the

capabilities of different carbon materials have not been explored yet. Thus, while the best candidates and/or the required properties that enable the optimization of these systems are still uncertain, the potential impact of METland® cannot be estimated. In addition, little can be deduced from literature so far because the studies about electroactive bacteria and materials properties are still in their infancy. First, the nature of bacteria extracellular electron transfer (EET) mechanisms involved in METs is still controversial [11]. Second, despite numerous bacteria-electrode interactions have been described in METs [12-17], little is undoubtedly known about the performance-determining electrode properties. This must be due to the complex nature of carbon materials, showing a wide range of intercorrelated properties, and the lack of systematic studies analyzing the effect of only a given electrode property, configuration, etc. In this sense, whereas some authors point out that the electroconductivity may be crucial for effective direct electron transfer (e-transfer) from bacteria to carbon (graphitic) matrices [18], what has been referred to as "geoconductor" mechanism, others suggest that this reaction primarily needs the mediation of electroactive oxygen surface groups [19]. Because the transferred electrons can be stored (on carbon basal planes or chemical bonds) and reversibly exchanged in biogeochemical processes, both e-transfer mechanisms have been associated to the so-called "geocapacitor" and "geobattery" behaviors, respectively [18]. Finally, most of the studies deal with MFCs [13-16], aiming at generating electrical power, so it is generally believed that the conductivity is the desired property of electrodes to optimize the microbial activity in METs [13-16]. Hence, systematic studies on the influence of the carbon material and its properties in METland® and other METs are necessary.

On the other hand, environmental concerns arise from the utilization of large amounts of carbon materials in full-scale METland® and other METs. In this context, the replacement of highly conductive carbon materials obtained from fossil resources, by those derived from renewable wastes, biomass and natural polymers, constitutes a hot topic of circular economy and big challenge among the scientific community [20-25].

Given the lack of fundamental knowledge on the influence of carbon properties in METs performance and e-transfer mechanisms; and the need of more sustainable biofilter materials for large-scale applications, in this work, the potential application of distinct carbon materials for wastewater treatment in METland® was investigated for the first time. Special attention was paid on the physicochemical and electrochemical characterization of these materials to find out properties-performance correlations and more meaningful conclusions. We demonstrate that the electrical conductivity is not the property determining optimal EET and biodegradation performance, but it governs the current production in these microbial electrochemical systems. Interestingly,

electroconductive biochar, exhibiting a large number of electro-active functional groups, revealed itself as the most efficient and sustainable biocompatible material for promoting microbial EET. Furthermore, we first propose the continuous regeneration of electroactive e-accepting quinone functionalities on biochar by anodic polarization to promote or modulate the biodegradation performance of carbon biofilters. All these results are considered to greatly progress the understanding of the e-transfer mechanisms on carbon surfaces through the geoconductor and geobattery mechanisms.

2. Experimental

2.1 *Bed materials*

The graphite (G) and the coke (C) were provided by METfilter SL. (Spain) The biochar (QB) was produced from Quercus wood by Piroeco Bioenergy S.L. A siliceous gravel (Azulejos Manchegos S.L., Spain) was used as a non-conductive material (NC). All the materials had a granular structure with a particle size ranging between 6 to 12 mm.

2.2 *Characterization of bed materials*

The surface morphology of the materials was studied by scanning electron microscopy (SEM), using a JSM-840 JEOL microscope working at 15 kV. X-ray diffraction (XRD) measurements were performed in a KRISTALLOFLEX K 760−80F diffractometer (Bruker D8-Advance) by using a Ni-filtered Cu Kα radiation (λ = 1.5416 Å) generated at 40 kV and 40 mA. Diffraction data points were recorded stepwise within 2θ = 10-60° at a scan rate of 0.56 or 0.83°/min, for the biochar or the rest of samples, respectively, with a scan step of 0.05° in 2θ. The crystallite dimensions (*Lc* or *La*), were calculated from the full width at half maximum (FWHM) of (002) and (10) reflections, respectively, by using the Scherrer's equation [26]. Raman spectra were recorded on a Jasco NRS-5100 dispersive system using a frequency-doubled Nd:YAG 532 nm laser, with a maximal spectral resolution of 1 cm^{-1}, and a Peltier cooled CCD detector. Electrical conductivity measurements were carried out by using a Lucas Lab resistivity equipment with four probes in-line. The samples were dried under vacuum for 24 h and shaped into pellets of 0.013 m diameter by applying a pressure of $7.4 \cdot 10^8$ Pa.

The porous texture was characterized by N_2 adsorption-desorption at -196 ºC and by CO_2 adsorption at 0 ºC (in the case of microporous samples), using a Quadrasorb-Kr/MP (Quantrachrome Corporation) apparatus. Samples were previously outgassed for 6 h at 150 ºC under vacuum. From the N_2 adsorption/desorption isotherm, the specific surface area (S_{BET}) was calculated using the BET equation [27]. The micropore volume (Vt) and the external surface area (At) were determined using the t-

method. The mesopore volume (V_{mes}) was calculated as the difference between total pore volume ($V_{0.995}$, volume at relative pressure of 0.995) and micropore volume [27]. The narrow micropore volume (V_{CO2}) and the narrow micropore surface area (S_{CO2}) were estimated for the biochar by applying the Dubinin-Radushkevich equation to the CO_2 adsorption isotherm [27]. The pore volume and dimensions were further characterized by Hg intrusion-extrusion porosimetry, using a PoreMaster 60-GT porosimeter (Quantachrome Instruments) with applied pressures from 6.84 to 408330 kPa. The Washburn equation was utilized to relate the applied pressure with the pore diameter [28].

The surface chemistry of the carbon materials was analyzed by X-ray photoelectron spectroscopy (XPS) in a K-Alpha spectrometer (Thermo-Scientific) with MgKα radiation (1253.6 eV). For the analysis of the XPS peaks, the C 1s peak position was set at 284.5 eV and used as reference to stablish the binding energy of the other peaks. The amount and nature of oxygen surface groups present on the carbon materials were studied by temperature-programmed desorption (TPD) experiments in a simultaneous TGA/DSC 2 equipment (Mettler-Toledo) coupled to a mass spectrometer (ThermoStar GSD 301 T, Pfeiffer Vacuum). In these experiments, around 20 mg of the carbon sample were heated up to 1000 ºC at 20 ºC/min under a He flow rate of 100 mL/min. Upon heating, surface oxygen groups on carbon materials decompose producing CO and CO_2 at different temperatures as a function of their thermal stability [35]. The quantification of the evolved CO and CO_2 groups was done by using a calcium oxalate monohydrate calibration and considering the CO disproportionation.

The microbial electrochemical response was studied by cyclic voltammetry in a H-type cell. Three different granules (one of each conductive materials) of ca. 1 cm^2 were externally connected and used as working electrodes in the same anodic chamber. The electrode potentials were referred against an Ag/AgCl/Cl^-(sat.) electrode immersed in the chamber. This contained 200 mL of fresh water medium with 20 mM acetate as electron donor. Cyclic voltammetry of each granule was sequentially performed, at 10 mV/s, just after inoculation (t = 0) with 20 mL of Geobacter sulfurreducens pure culture (OD = 0.6); and after polarization of the granules at 0.2 V for 7 days (t = 7). Further details can be found in the Supplementary Data (SD) file (Fig. S1).

2.3 *Design and construction of biofilters*

Eight laboratory-scale up-flow biofilters were constructed to determine the influence of the bed materials in the treatment of urban wastewaters. Four of the systems were constructed with a single material/electrode and operated as a snorkel configuration (see Fig. S2A in the SD). This configuration did not allow the conversion of microbial metabolism into electrical current to be monitored, since the anode and cathode were not differentiated. The dimensions of the snorkel biofilters were 24 cm high

and 3 cm internal diameter, with a total bed volume of 170 cm^3 and a hydraulic volume of 100 mL. Each biofilter outlet for the effluent was located at the top, which maintained the water level below the bed's surface.

On the other hand, the other systems were assembled with a three-electrode configuration, allowing to harvest electrochemical information about the process (see Fig. S2B in the SD). These hybrid biofilters hosted one of the electroconductive materials as anode of 78 cm^3 (working electrode); a bed of 58 cm^3 of pyrolyzed coke used as cathode (counter electrode); and a $Ag/AgCl/Cl^-$ (sat.) reference electrode buried in the anodic bed for its polarization at a given potential. In each system, the anode and the cathode were separated with 14 cm^3 of inert gravel; and they were externally connected through buried graphite rods (1.5 cm × Ø 0.2 cm, Sofacel) used as current collectors. In the case of the anode, two buried graphite rods were used to ensure homogenous polarization of the particles bed. This condition was confirmed by the constant potential of various granules, registered in different parts of the bed, against the reference electrode. Both, the anode potential and electrical current were monitored by using different NEV-4 potentiostats (Nanoelectra S.L., Spain). Finally, a similar system, but without current collectors and reference electrode, was constructed as a control with the gravel material.

2.4 *Operation of the biofilters*

The different systems were operated in parallel to study the influence of several parameters, including the bed material, the nature of wastewater (synthetic vs. real urban wastewater), the hydraulic retention time and the polarization of bed material at different potentials. In the case of synthetic wastewater, biofilters were operated under batch and continuous mode (pulse fed, HRT = 3.3 days) under snorkel configuration. On the other hand, for real urban wastewater the biofilters were operated in continuous mode, fed by pulses, with (i) two different organic loading rates (OLR= 170 mg/L and 890 mg/L), (ii) two different hydraulic retention times (HRT = 4 and 2 days) and (iii) three different anode potentials (short circuit (non-polarized), 0.4 V and 0.6 V vs. $Ag/AgCl/Cl^-$ (sat.)). In this mode, the measurements started (time of experiment = 0 days) after the systems were stabilized, i.e. when the pollutant concentration at the outlet remained steady (error < 5 %) for 3 subsequent days. This condition was accomplished by subsequently passing and replacing three different aliquots of the different wastewater, enabling adsorption equilibriums to be reached. Therefore, adsorption effects on the reported results can be neglected. The real urban wastewater was pretreated in an Imhoff tank, in the WWTP of Carrión de los Céspedes (Sevilla, Spain), the chemical characterization appears in Table S1. The biofilters were operated under continuous mode for 84 days (12 weeks). In all cases, the temperature was maintained at 30 ºC in a temperature-controlled room.

2.5 *Physical, chemical and statistical analyses*

Samples were taken daily at the inlet and the outlet of the biofilters. Acetate concentrations were determined by HPLC coupled to a diode array detector (Varian). The chemical oxygen demand (COD) was analyzed following a standard method [29]. The theoretical oxygen demand (ThOD) of acetate solutions was determined assuming the complete oxidation of carbon atoms, according to the following stoichiometric equation:

$$C_2H_4O_2 + 2O_2 \rightarrow 2CO_2 + 2H_2O$$

Removal efficiencies were calculated as percentage of the inlets. Removal rates were obtained from the inlet-outet difference as mol or grams per cubic meter of bed material per day. The data provided in the bar graphs (see Fig. 4 and 5) correspond to the average value of 5 measurements taken, during 5 successive days, after a steady response was reached. In order to discern the true effect of the bed materials for each operation condition, statistical procedures were conducted with these 5 measurements using R software (R Core Team 2013) and R-comander package (Fox 2005). The standard deviation of these measurements is included in these bar graphs. Variance analyses (ANOVAs) were used to determine statistical significance (p-value < 0.05) in the performance differences among the different bed materials.

3. Results and discussion

3.1 *Characterization of biofilter materials: physico-chemical properties, electroconductivity and EET*

The textural properties of the materials may play a key role on the microbial activity and/or colonization, so they were characterized by SEM, Hg porosimetry and gas adsorption. The non-electroconductive (NC) siliceous gravel showed a smooth surface from milli- and micro-scale (Fig. 1A) to nano-scale, what was confirmed by the negligible volume of Hg intruded (Fig. 1E and Table 1) or N_2 adsorbed (Table 1) in this material. These features are in line with the geological origin of this type of rocks, which were formed by weathering and erosion.

By contrast, all the carbonaceous materials presented a differently rough and porous surface. The graphite shows a heterogeneous surface (Fig. 1B), combining relatively smooth with ridged regions of wrinkled sheets and cracks of ca. 1-10 µm. The coke granules present a very abrupt morphology with large crater holes (Fig. 1C). Finally, the biochar exhibits a developed porous structure (Fig. 1D), with regular pores of cylindrical morphology and different dimensions. In particular, a series of big channels of 50-100 µm, surrounded by several pores of around 1-5 µm (Fig. 1D1), prevail at this scale in the biochar. In addition, the magnification of the inner walls at the bigger channels revealed the presence

of a large amount of well-arranged and defined transverse pores of ca. 1-2 µm (Fig. 1D2), that seem to interconnect the channels. This extraordinary pore structure comes from the distinct channels and/or vascular cells present in the original plant [22].

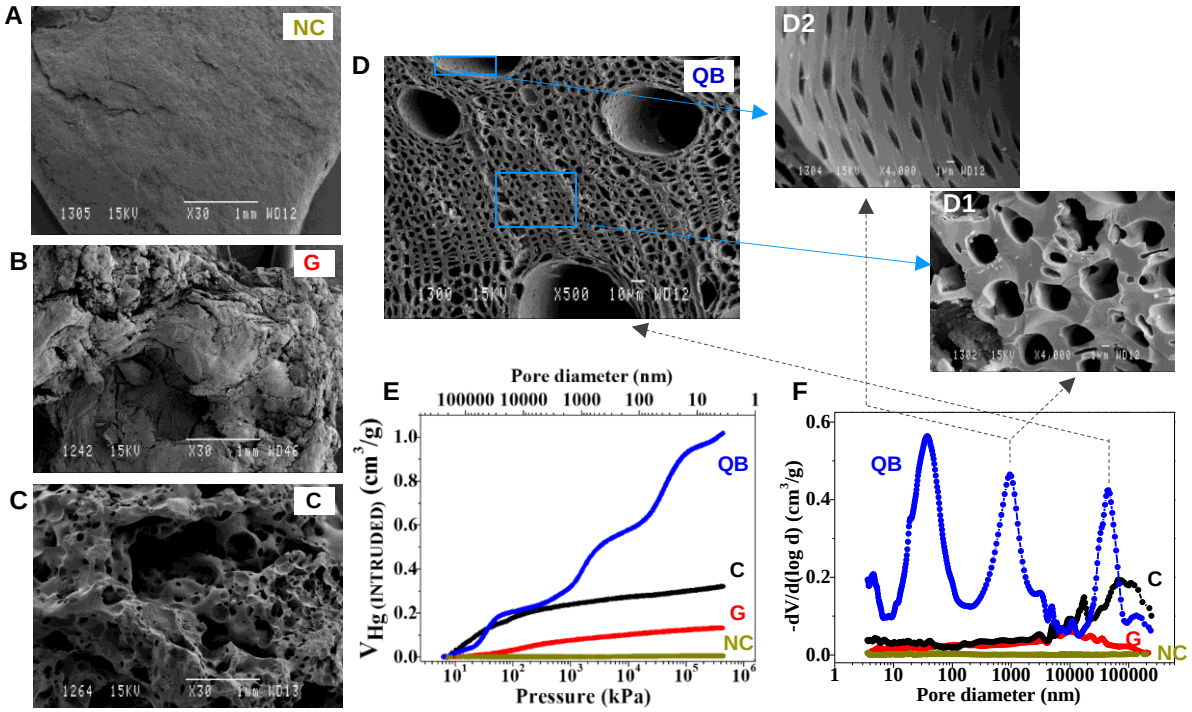

Figure 1. A-D) SEM micrographs; E) Hg intrusion porosimetry and F) the derived pore size distribution of the bed materials before being used as electrogenic biofilters. NC, non-conductive gravel; G, graphite; C, coke; QB, Quercus electroconductive biochar.

Table 1. Textural, structural and chemical parameters of graphite (G), coke (C) and - Quercus electroconductive biochar (QB) before and after being used, polarized at 0.6 V, as electrogenic biofilter beds.

	N_2 isotherms				CO_2 isotherms		Hg porosimetry		XRD		Raman		TPD		
Biofilter	S_{BET} [a] m^2/g	$V_{0.995}$ [b] cm^3/g	Vt [c] cm^3/g	V_{mes} [d] cm^3/g	S_{CO2} [e] m^2/g	V_{CO2} [f] cm^3/g	V_{Hg} [g] cm^3/g	ρ [h] g/cm^3	0 0 2 [i] °2θ	*Lc*/*La* [j] Å	ν_G [k] cm^{-1}	$\Delta\nu_G$ [l] cm^{-1}	CO_2 [m] µmol/g	CO [n] µmol/g	O [o] µmol/g
G	< 1	0.001	0.000	0.000	---	---	0.133	2.153	26.577	628/653	1579	21.3	45	19	109
G0.6	< 1	0.004	0.000	0.000	---	---	0.135						---	---	---
C	< 1	0.001	0.000	0.001	---	---	0.322	1.781	25.404	22/43	1599	57.5	49	38	178
C0.6	< 1	0.002	0.000	0.001	---	---	0.306						---	---	---
QB	250	0.135	0.120	0.010	550	0.187	1.019	1.610	23.520	10/20	1587	77.2	683	1230	2596
QB0.6	210	0.117	0.098	0.012	526	0.179	0.794						---	---	---

[a] Specific surface area from BET model. [b] Total pore volume at P/P^o = 0.995. [c] Micropore volume from *t*-method. [d] Mesopore volume. [e] Specific surface area and [f] Ultra-micropore volume from Dubinin-Radushkevich. [g] Total Hg intrusion volume. [h] Material density. [i] Position of the 002 peak. [j] Calculated crystallite dimensions of the graphite crystalline structure. [k] Position and [l] width of the G band. [m] Integrated CO_2- and [n] CO-evolving oxygen surface groups from TPD. [o] Total surface oxygen O = CO + 2 CO_2.

The porosity analysis by cumulative Hg intrusion curves (Fig. 1E) clearly indicates that the Quercus biochar can intrude a considerably larger volume of Hg than the other materials. As shown in Table 1, the calculated total pore volume (V_{Hg}) of the materials remarkably increases in the order NC << G < C < QB up to ca. 1 cm^3/g, whereas their density increases in the opposite order from about 1.6 to 2.7 g/cm.

From the derived pore size distributions (Fig. 1F), it can be inferred that the graphite presents macropores (pore diameter (d) > 50 nm) with a wide spectrum of dimensions and the coke material mainly contains pores above 10 µm. Moreover, these materials contain no micropores (Vt) (d < 2 nm) and mesopores (Vmes) (2 < d < 50 nm) (see N_2 isotherms-Fig. S3 in the SD), thus, showing a very low specific surface area (S_{BET}) that is comparable to that of gravel (Table 1). By stark contrast, the pore size distribution of the electroconductive biochar revealed three defined peaks, with maximums at ca. 37 nm, 950 nm and 44.5 µm (Fig. 1F). This porosity well agrees with the features found by SEM (Figures 1D, 1D1 and 1D2). In addition, this material presents a large volume of micropores (Vt) and, mostly, of narrow micropores (V_{CO2}) (ultramicropores, d < 0.7 nm), leading to a specific surface area (ca. 550 m^2/g) much larger than the other carbon materials (Table 1). Furthermore, the N_2 isotherm also revealed the presence of some mesopores in this sample (Table 1), what is in line with Hg porosimetry (Fig. 1E). Hence, the electroconductive biochar exhibits a unique hierarchical pore architecture gathering ultramicro-, micro-, meso- and macro-pores.

The structure of the bed materials was analyzed by XRD and Raman. A detailed compilation of all the spectral parameters can be found in the SD (Tables S2 and S3), but most important ones are included in Table 1. The X-ray diffractograms of the gravel (see Fig. S4) indicated that this material is mainly formed of α-quartz (SiO_2) microcrystallites. In the case of the carbon materials, two characteristic diffraction peaks appear centered at around 2θ = 23 - 27° and 42 - 44° (Fig. 2A). The first peak is related to the vertical ordering/stacking of graphene sheets aligned along the (002) plane in graphite; whereas the second one is associated to the horizontal arrangement of these sheets along the (100) plane [30,31]. In the case of the graphite, the center (2θ) of these peaks greatly approaches that found for highly-ordered pyrolytic graphite (HOPG) at 26.53° and 42.44°, respectively (see Tables 1 and S2). This involves that the lattice parameters (d-spacings along with *c*/*a* axis) of this sample are close to those expected for graphite crystals, thus, reflecting its superior structural order. As observed in the inlet of Fig. 2A and Table 1, the diffraction peaks for the coke and, in more extent, the biochar separate from those of the graphite. On the other hand, the narrower these peaks are, the larger the *Lc*/*La*

dimensions of these crystals. The size of crystallites in the graphite were calculated to be ca. 630-650 Å, and greatly decreased to 20-40 Å and 10-20 Å for coke and biochar, respectively (Table 1).

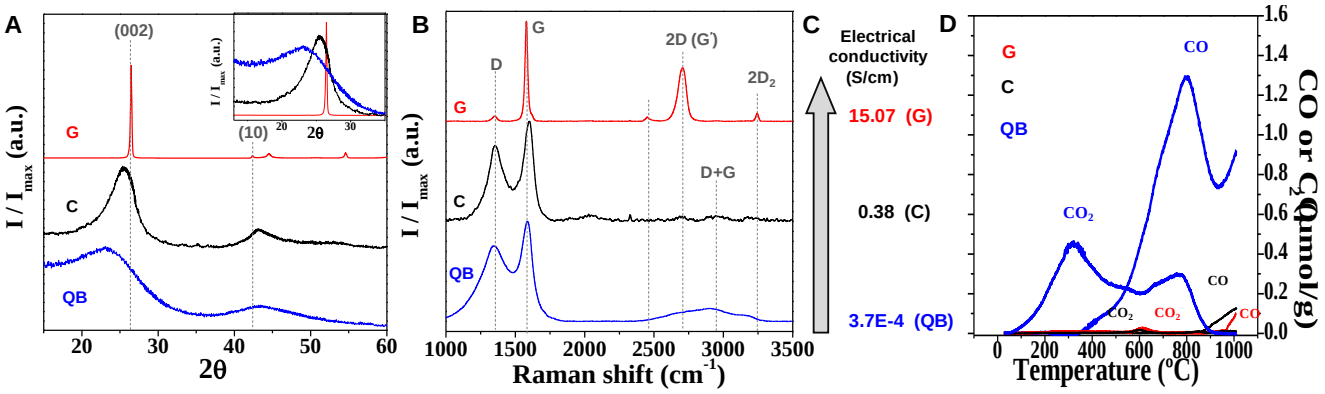

Figure 2. Normalized X-ray diffractograms (A) and Raman spectra (B); the electrical conductivity from 4 probe measurements (C); and TPD (D) of the carbon materials used as electrogenic biofilters. NC, non-conductive gravel; G, graphite; C, coke; QB, Quercus electroconductive biochar.

Respect to Raman characterization, the observed two main bands of the first-order spectrum of the carbon materials (Fig. 2B), called the D-band (~1340-1360 cm^{-1}) and the G-band (~1579-1599 cm^{-1}), provide information on the structural defects or graphitic order, respectively, related to the degree of two-dimensional orientation of the crystalline units. On the other hand, the overtone of the D band in the second order spectrum, called the 2D-band (~2700 cm^{-1}), has been associated to the degree of three-dimensionally graphitic orientation [31]. In the case of graphite, the G-band position and width, comparable to the values found for HOPG (νG = 1578-1582 cm^{-1} and $\Delta\nu G$ = 17-20 cm^{-1}) [32,33], the relative low-intensity and narrow D-band, and the high relative intensity of the 2D-band are all characteristic of a graphitic material (Table S3). On the contrary, the wider D, G- and 2D-bands, obtained for coke and Quercus biochar reflect their more defective structure, which is exacerbated for the later. All these results point out the poorer crystallinity (structural order) of the coke and, specially, the biochar, and can be well correlated with their electrical conductivity (Fig. 2C). Thus, the studied graphite shows a high conductivity of around 15 S/cm, which is in the order of these structurally ordered materials [34]. Interestingly, this conductivity is ca. 40 and more than 40000 times higher than those of coke and biochar, respectively.

The surface oxygen content of the carbonaceous samples, from XPS analysis, was found to be 1.7; 6.5 and 16.7 wt.% for the graphite, coke and biochar, respectively (Table S4). This trend is in line with the quantified evolving groups during TPD experiments (Table 1). From the TPD profiles (Fig. 2D), it can be clearly deduced that the electroconductive biochar presents a remarkably richer surface chemistry. Particularly, this material is by far characterized by a large CO evolution from 500 ºC, with

a hump and a maximum at ca. 700 and 800 ºC, respectively, which have been assigned to phenol and quinone/carbonyl functionalities in carbon materials [35]. These oxygen groups have been found to be electroactive [36]. Moreover, it contains a considerable amount of oxygen surface groups evolving as CO_2 between 150-400 ºC, attributed to carboxylic-like functionalities, and some other groups, like anhydrides and lactones, at higher temperatures [35]. To summarize, whereas the graphite and coke exhibit a higher conductivity because of their superior crystalline structure (mainly in the former case); the electroconductive biochar displays a higher surface area, a hierarchical pore architecture and a richer surface chemistry, including a large amount of electroactive oxygen functionalities.

The microbial EET capability of the different materials was studied by cyclic voltammetry. Figure 3 compares the voltammetric profiles of a single granule of each material before inoculation and after 7 days of promoted (potentiostatic) biofilm growth. Just after inoculation (grey lines), the CV revealed how the different materials display a redox couple attributed to surface e-transfer (acetate - carbon electrode) mediated by cytochrome C of bacteria [37]. In all cases, the current density and/or charge involved in this EET increased after biofilm growth (colored lines). However, evident differences can be observed among the tested materials. First, the voltammograms obtained from electroconductive biochar (Fig. 3C) were comparatively more tilted than those from graphite and coke (Fig. 3A-B); a response that can be related to the inherent lower electroconductivity of the former material (Fig. 2C). Second, the shape and current density of these electrochemical processes, including its relative increase after biofilm growth, depended on the nature of the biofilter material. Specifically, the coke and the graphite show quite similar straight voltammograms with broad peaks and relative increments of e-transfer capability after biofilm growth (Fig. 3A-B). Nevertheless, the current density of graphite is one order of magnitude higher.

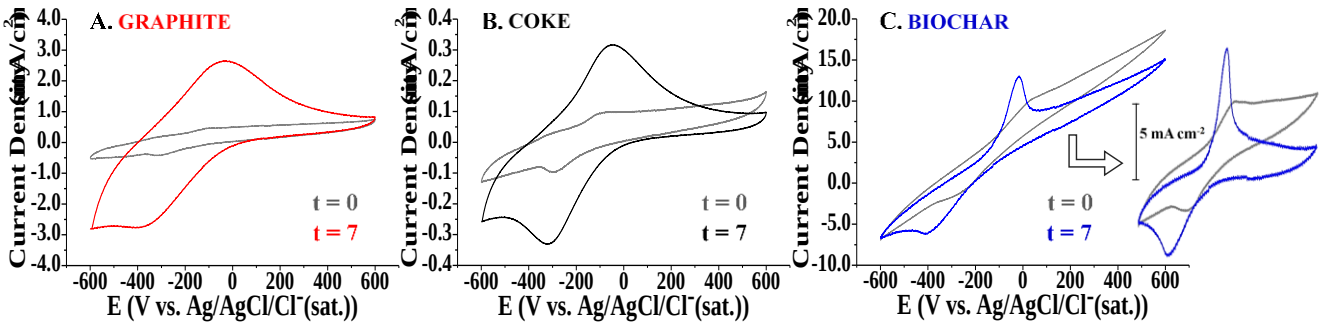

Figure 3. Steady-state cyclic voltammograms of a single granule of the different biofilter materials just after inoculation (Geobacter sulfurreducens) (t = 0) and after polarization at 0.2 V (vs. Ag/AgCl/Cl^- (sat.)) for 7 days (t = 7) to promote biofilm growth; scan rate = 10 mV/s; fresh water medium, 20 mM acetate.

On the other hand, the electroconductive biochar (Fig. 3C) exhibited much higher voltammetric currents throughout all the analyzed potential window in comparison with the rest of tested materials, even just after inoculation. This is assigned to the higher specific surface area of electroconductive biochar (Table 1). In this case, however, the relative increase in current density after biofilm growth seemed to affect to a narrower potential window, leading to more intense and define peaks. As a result, the charge associated to the e-transfer on the biochar was considerably larger than in the case of graphite and coke. This may be due to a property unlike conductivity.

3.2 *Biofilters performance for treating wastewater using different electroconductive bed materials*

The mere presence of electroconductive material has been shown to stimulate microbial biodegradation of pollutants in a number of studies [5-8]. Thus, we decided to explore such a response using the different materials (graphite, coke, electroconductive biochar and gravel as non-conductive control material) for constructing the biofiltering bed.

3.2.1 *Biofilter performance for treating synthetic wastewater*

The four biofilters were independently operated up-flow with acetate-based synthetic wastewater under batch or continuous mode. The initial concentrations of acetate were different depending on the operational mode. In batch mode, the initial concentration of acetate was 40 mM, showing a ThOD of 1279.4 mg/L. When the biofilters were operated in continuous mode, the initial acetate concentration was 20 mM (ThOD = 639.7 mg/L), to mimic the organic compound content of a standard urban wastewater. Regardless the operating mode, the residual concentration of acetate in the effluent was lower in those biofilters whose bed was made of electroconductive material (Figure 4). Nevertheless, despite its lower conductivity, the electroconductive biochar was the most efficient material for biodegrading acetate under any operating mode. Particularly, in batch operation (Fig. 4A) it removed 100 % of the acetate in 2 days (4.14 mol acetate $m^{-3}d^{-1}$), working at double rate than the other tested conductive materials; in contrast, biofilter made of inert gravel only removed 25 % of acetate during the same period.

When operated under continuous mode (Fig. 4B), the electroconductive biochar biofilter showed also removal efficiencies close to 100 % after 2 days, implying removal rates of 2.79 mol acetate $m^{-3}d^{-1}$. In this case, however, the other two electroconductive materials were not able to remove more than ca. 70 % of the acetate even after 4 days of treatment (1.0-1.2. mol acetate $m^{-3}d^{-1}$) and the gravel was totally inefficient under these conditions.

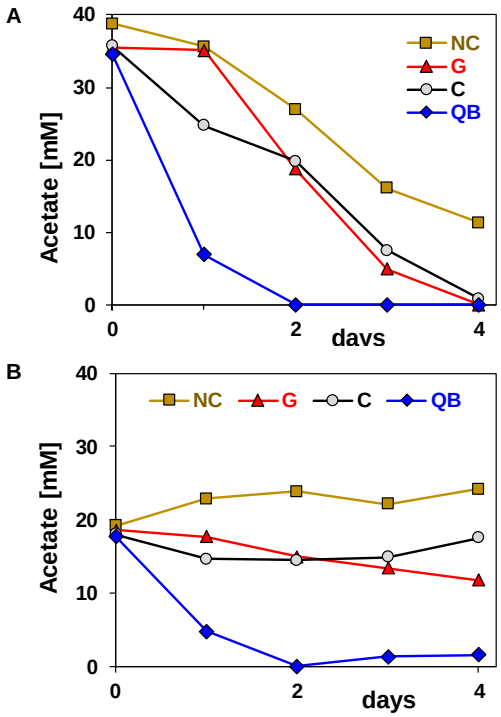

Figure 4. Evolution of acetate concentration in the biofilters operating in (A) batch and (B) continuous (HRT = 3.3 days) mode. NC, non-conductive gravel; G, graphite; C, coke; QB, Quercus electroconductive biochar.

3.2.2 *Biofilter performance for treating real urban wastewater*

In order to evaluate the performance of the biofilters under a more real scenario, they were fed with a real urban wastewater under a continuous mode. Moreover, in real scenarios the HRT and the OLR are critical parameters, so their influences were analyzed. Statistical test revealed significant differences ($p < 0.05$) in the COD from effluents at all OLRs and HRTs tested.

Respect to the effect of HRT, as expected, the effluent COD discharges decreased, and the removal efficiencies increased, with the HRT; i.e. by extending the biofilter-wastewater contact time. In the case of a 170 mg/L COD influent, for example, the performances of both the coke and graphite biofilters were within the limits of discharge of the European Directive 91/271/CEE [38] at a HRT of 4 days. In contrast, biofilters made of gravel required an HRT above 4 days to fulfill the limits. Interestingly, only the electroconductive biochar biofilter fulfilled the requirements of the directive for COD at HRT as low as 2 days. Considering the more practical benefits of minimizing the HRT, the following studies exploring both the influence of the OLR or the material polarization were carried out at a HRT of 2 days.

Regarding the influent concentration (OLR), real urban wastewaters typically show a variable nature according to human activity along the day. To quantify the robustness of the system to variations in the organic load, the biofilters were fed with influents showing 5-fold differences in COD levels: 170 and 890 mg/L (Figure 5). As mentioned above, when the influent COD was 170 mg/L the only system that fulfilled the requirements of the directive for COD discharge was the electroconductive biochar biofilter, which actually removed COD at ca. 31 g $m^{-3}d^{-1}$.

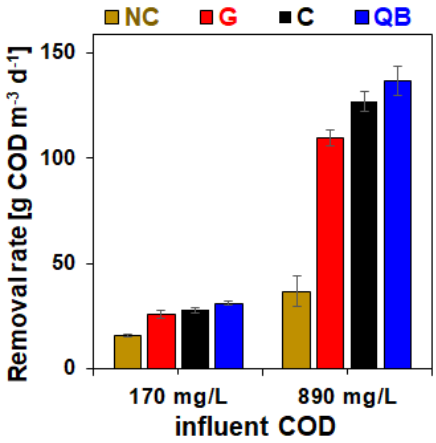

Figure 5. Average COD removal rate including ± standard errors in each biofilter without polarization, referred to HRT = 2 days and two different OLRs in urban wastewater. NC, non-conductive gravel; G, graphite; C, coke; QB, Quercus electroconductive biochar.

Under higher COD loads (890 mg/L), the electroconductive biochar was also the biofilter with the best performance (Fig. 5). Moreover, the removal rate was increased more than 4-fold in the different electroconductive biofilters, specially up to 137 g $m^{-3}d^{-1}$ for the biochar, while the gravel biofilter did not remove more than ca. 37 g $m^{-3}d^{-1}$. Interestingly, in spite of the high electroconductive nature of the graphite, its performance was worse than that of coke. Hence, a remarkable conclusion is that the conductive character of the carbon biofilters seems to be responsible of the their much better performance than gravel, but something different to conductivity may govern the performance among the carbon biofilters to explain the greater response of the poorly conductive biochar.

3.2.3 *Biofilter performance for treating real urban wastewater using polarized beds*

With the aim of exploring the role of the electroconductive bed for accepting electrons from microbial metabolism, we constructed three independent biofilters with anodic beds subjected to electrochemical control by polarizing them at either 0.4 V or 0.6 V (vs. Ag/AgCl/Cl^- (sat.)) and the produced current was monitored. For comparison purposes, the biofilters were also operated without polarization (NP) under short circuit mode. The systems worked under continuous mode (HTR = 2 days), fed by pulses,

with a high COD load influent (ca. 800 mg/L). Figure 6 compilates the results in terms of biodegradation and current production of the different wastewater treatments.

First, in respect of the biodegradation performance, the analysis of variance (ANOVA) revealed significant differences ($p < 0.05$) among the tested materials. As a general response, without polarization (NP bars in Fig. 6A), none of the studied biofilters was able to fulfill the discharge limits at such high organic load. On the other hand, the anodic polarization of the electroconductive biofilters (0.4 or 0.6 V) remarkably enhanced their COD removal capacity (Fig. 6A). In contrast, the gravel biofilter performance was not affected by polarization, what is assigned to its non-electroconductive nature. Hence, electroconductivity was found a necessary property to optimize the microbial activity of the biofilters by external polarization.

Particularly, the polarized electroconductive biochar was the most effective biofilter for cleaning-up wastewater among all the tested materials and conditions (Fig. 6). At 0.4 V, the polarization of the electroconductive biochar bed reduced (by 3.5-fold) the COD level at the effluent down to 100 ppm (Fig. 6A), fulfilling the regulative policy. In this case the COD removal efficiency greatly increased from 56 to 87 % (average value in Fig. 6C) and the removal rate from 112 to 176 g $m^{-3}d^{-1}$ (Fig. 6B). For the other two conductive biofilters, made of coke and graphite, the removal efficiency just increased in 6.1 and 19.4 % (up to 53 and 58 %, average values in Fig. 6C), respectively; what was not enough, however, to fulfill the requirements of the directive for COD levels (Fig. 6A).

A further increase in the electrode potential up to 0.6 V resulted in a better performance of the conductive biofilters by increasing the COD removal rates (Fig. 6B). In this case, however, the most electroconductive biofilters (made of coke and graphite) experienced the largest relative increments in COD removal efficiency, 27 % and 18 %, respectively (vs the efficiency at 0.4 V). Nevertheless, the removal efficiency of the biochar (92 % average, Fig. 6D) was still considerably higher than those of coke and graphite (80 and 75 % average, respectively, Fig. 6D). These effects were also observed for the removal rates (Fig. 6B), reaching a maximum degradation rate of 185 g $m^{-3}d^{-1}$ in the case of electroconductive biochar. As a result of these different performances, the effluent from the biochar biofilter (64.13 ± 5.3 mg/L COD) was again the only one not exceeding the discharge limits (Fig. 6A). Hence, by simple modulation of the potential, the electroconductive biochar can clean up urban wastewaters even with influents load as high of ca. 800 mg/L COD. Interestingly, such a higher biodegradation performance of the electroconductive biochar biofilter suggests some kind of EET process that was experimentally confirmed by the e-transfer capability between bacteria from genus Geobacter and this material (Fig. 3).

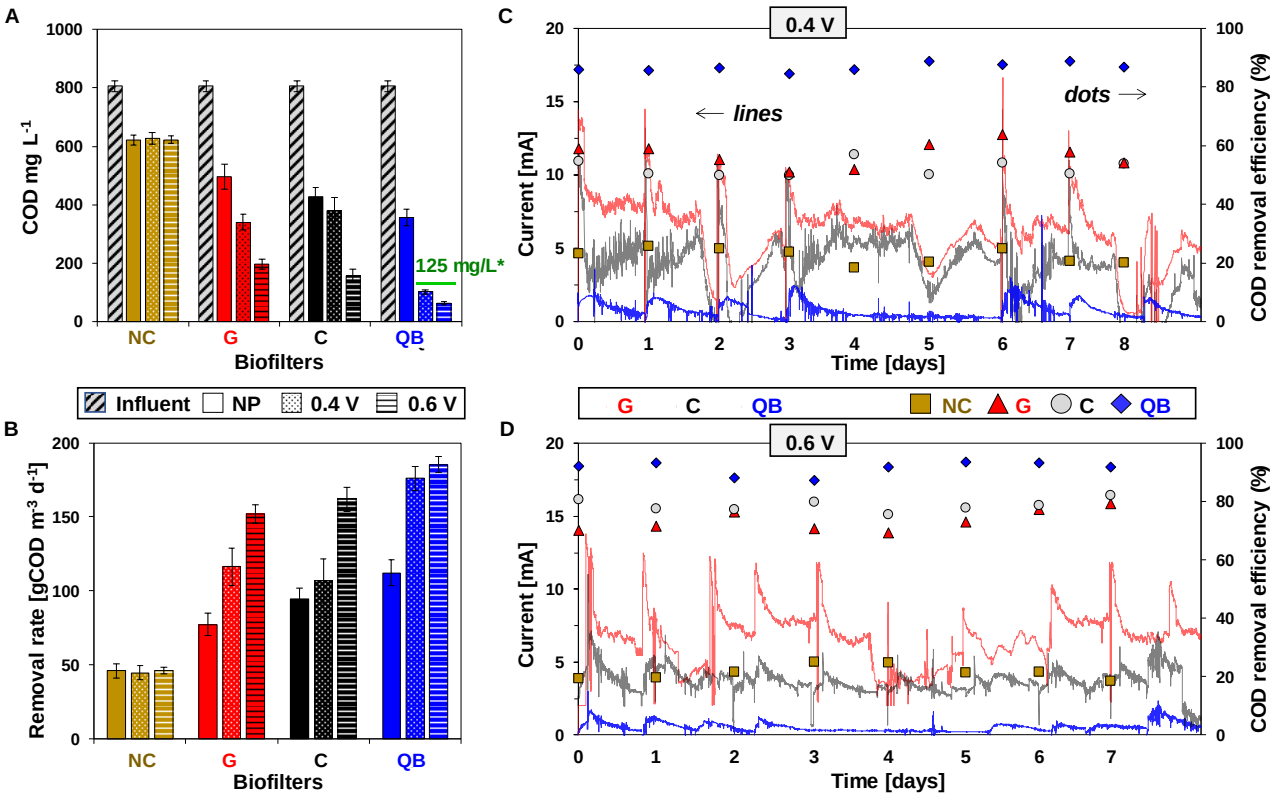

Figure 6. (A) Average effluent COD (showing discharge limit* [38]); and (B) COD removal rate, including ± standard errors, in each biofilter submitted to different polarization conditions (NP = non-polarized, in which the open circuit potentials were: -420 mV, -427 mV and -429 mV for the graphite, coke and biochar, respectively). (C-D) Evolution of the COD removal efficiency (dots) and the microbial electrical current (lines) while treating real urban wastewater using electroconductive biofilters anodically polarized at (C) 0.4 V and (D) 0.6 V (vs. Ag/AgCl/Cl^- (sat.)). Influent COD = 800 mg/L; HRT = 2 days. NC, non-conductive gravel; G, graphite; C, coke; QB, Quercus electroconductive biochar.

Second, production of significant electrical current was detected and monitored during the polarization assays (Fig. 6C-D). Interestingly, the progressive addition of new inlet media caused an immediate increase in the electrical current production due to the microbial response. This current-production profile was similar for all systems regardless the material used for the bed. Thus, using the polarized materials as electron acceptors confirmed the conversion of the microbial metabolism into transferable electrons.

In particular, by polarizing at 0.4 V the monitored average currents were 0.78, 3.65 and 6.13 mA for the biochar, coke and graphite biofilters, respectively (Fig. 6C). This trend in current production seems to agree with the increasing conductivity of these materials (Fig. 2C). With an increment of the

electrode potential to 0.6 V, the average current in coke and graphite biofilters slightly increased to 3.74 and 6.69 mA, respectively, in contrast with the practically unaffected current from biochar (Fig. 6D). From all these results, it can be concluded that the raise in the electrode potential at higher values (at least from 0.4 to 0.6 V) to increase the COD removal capability and the current production was less effective for biochar, the least conductive carbon biofilter. Another important conclusion is that the current production in these polarized bed-like biofilters is not directly correlated to COD removal, which generally increases in the opposite order, this is graphite < coke < biochar, (Fig. 5-6).

Regarding that the soluble electron donor (organic matter) present in wastewater is not a limiting factor, this fact could be explained by different reasons. Firstly, previous reports suggested the presence of alternative biodegradation pathways, using methanogens [39,40] or sulfate-reducing bacteria [40], which do not contribute to current production [41]. Secondly, part of these "lost" electrons could be utilized in the promotion of syntrophic metabolism by biochar-mediated Interspecies Electron Transfer [42-44]. Thus, Chen et al. (2014) proposed that the electrons can migrate from electron-donating to electron-accepting cells by inducing intrinsic charge differences between sections of biochar [42]. This intra-particle electron migration, however, cannot be measured as current. In this sense, the harvested current must be exclusively associated to the capability of the bed of carbon particles to move and extract the electrons from their surface to other particles and, finally, the current collector, i.e. to the inter-particle electron migration. Such ability must be directly related to the intrinsic conductivity of the material and its shape and conformation in the biofilter, i.e. the conductivity of the particles bed. This is line with Sun et al. (2017) [18], who suggested that the electrical conductivity may lead to a relatively longer-distance transport of electrons through carbon matrices. Hence, the most reasonable explanation could be a higher electrical resistance of the biochar particles bed. This agrees with the lower conductivity of the biochar respect to that of the coke and graphite (Fig. 2C), together with the insignificant effects on biodegradation by rising the potential of biochar biofilter from 0.4 to 0.6 V (Fig. 6).

On the other hand, although both galvanostatic (Fig. 6C-D) and voltammetric (Fig. 3) measurements reflect a greater microbial activity on biochar, they seem to diverge in the relative capability of the different materials for current production. It must be considered, however, that the experimental conditions in these measurements were substantially different. First, in the case of galvanostatic experiment, the nature of the e-donor (real urban wastewater) was much more complex, showing lower coulombic efficiencies (CE ca.10 % or below depending on the influent COD) [5] than the acetate-based medium (CE ca. 95 %) [45] used in voltammetry. Second, while the galvanostatic experiment was performed over a bed of granules, a single granule was used for voltammetric analysis. The fact

that greater currents are registered on biochar when using a single granule, and that the opposite occurs in the bed-like configuration, strongly supports the occurrence of higher current losses (resistance) among the particles of the biochar.

3.3 *Giving insight into the extracellular electron transfer to electroconductive carbon materials*

To understand the previous results, the nature of microbial electrochemical processes should be considered. Although the involved mechanisms are not fully understood, the e-transfer capability of carbon materials (e-acceptors) with bacteria has been generally attributed to their electroconductivity [18] and/or the presence and mediation of electroactive hydroquinone-quinone (HQ/Q) surface moieties [19]. See a proposed scheme of these processes in Figure 7.

On the one hand, the electroconductivity-based mechanism, recently referred to as the geoconductor behavior [18] involves a direct e-transfer to/from the carbon matrix (aromatic structure) and has been reported for carbons prepared at higher temperatures, i.e. minimizing the contribution of surface oxygen surface groups [18,46] Nevertheless, the promotion of direct interspecies electron transfer (DIET) for different syntrophic associations of microorganisms in soils has been assigned to the electrical conductivity in both low-conductive carbons, like biochar [42-44], and more conductive materials, like graphite [43]. Indeed, not only the conductivity but also the capability of the conjugated π-electron system of the condensed aromatic rings in carbon materials to accept/donate electrons (redox character) [47] may contribute in this mechanism.

On the other hand, the mechanism based on the HQ/Q reversible redox reaction was proposed to explain how biochars promote interspecies e-transfer in soils [19] acting as rechargeable reservoirs of bioavailable electrons, i.e. the so-called geobattery behavior [48]. However, these specific (HQ and Q) functionalities were not experimentally observed or quantified in most of these previous works. On the contrary, the TPD technique has been used in this work to quantify the amount of these groups [36]. Most of the CO-evolving groups in Fig. 2D, around 1000-1100 μmol/g, correspond to these types of functionalities. Then, it is reasonably to propose that the considerably greater e-transfer capability (Fig. 3) and higher biodegradation efficiency (Figures 4-6) observed for the much poorly conductive biochar is assigned to the larger amount of electroactive oxygen functionalities. Similarly, the slightly better performance of the coke compared to graphite, could be also explained by this mechanism (see the amount of CO-evolving groups in Table 1). Then, the bioelectrochemical response of the studied biofilters seems to be governed by the geobattery mechanism.

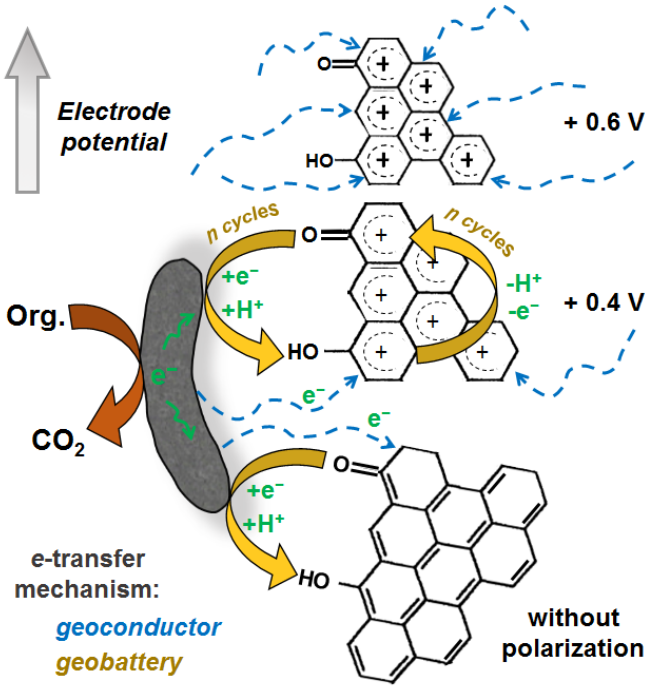

Figure 7. Scheme of the proposed geoconductor and geobattery e-transfer mechanisms between bacteria and carbon materials, emphasizing their possible modulation, externally, by polarization.

Concerning the kinetics of the process, it was reported that the direct e-transfer (geoconductor behavior) through carbon matrixes is three times faster than through HQ/Q processes [18]. However, this study did not consider the effect of the different material's electroconductivity on the reaction kinetics and, additionally it was carried out under abiotic conditions, by analyzing the electron exchange between carbon electrodes and dissolved species [18]. In contrast, both the higher acetate and COD removal-rates (Figures 4-6) obtained in biochar-made biofilters in this work suggest that e-transfer between carbon materials and bacteria is faster when mediated by HQ/Q functionalities

The enhancement in removal efficiency upon polarization observed for these electroconductive biofilters, together with the significant increase in the COD removal rates (Fig. 6B), is assigned to a stimulation of the biodegradation rate of microorganisms on these systems. It has to be considered that a polarization at 0.4 - 0.6 V (vs. Ag/AgCl/Cl^-) is remarkable, since the typical environment in anaerobic biofilters reach a very negative redox potential (ca. -350 mV vs. Ag/AgCl/Cl^-). Interestingly, our polarized biofilters may support bacterial growth able to exchange electrons with the material substrate at oxidative potentials as high as 0.6 V, a value which is not far from the value exhibited by oxygen (0.8 V vs. Ag/AgCl/Cl^-) in typical aerobic biological systems. As a result, by providing an electron acceptor with a high potential using electrochemical tools we may optimize the oxidation of the pollutants while avoiding the cost of supplying oxygen into the liquid phase.

This modulation of the e-accepting capability of the biofilter supports the occurrence of the geoconductor mechanism. Thus, the anodic polarization causes a depletion of π-electrons from aromatic rings that may favor their e-accepting capability from bacteria (see Fig. 7). Despite such electron extraction is expected to be easier at higher conductivity, the obtained results point out that the polarization at 0.4 V causes a much greater biodegradation promotion on the biochar (Fig. 6A and 6B). This effect could be explained by the electrochemistry of HQ/Q couple. In fact, several works on the electrochemistry of biomass-derived carbon materials report that 0.4 V (vs. Ag/AgCl/Cl^-) is a high-enough electrode potential to oxidize hydroquinone (HQ) groups into quinone (Q) ones [49,50]. Considering that these Q groups are the e-acceptors in the geobattery mechanism, the polarization at 0.4 V greatly augments the number of e-acceptors on the biochar and, therefore, its biodegradation ability. Furthermore, the HQ/Q is a well-known reversible redox couple, so that, once the bacteria transfer the electrons to the Q groups, and reduce them into HQ ones, the effect of the anodic polarization may restore again the quinone functionalities (as schematized in Fig. 7). From the experimental results, this cyclical regeneration of quinone e-acceptors by polarization is proposed to remarkably enhance the biodegradation rate and efficiency of the carbon material. Moreover, this e-transfer from bacteria to the continuously recycled quinones (geobattery mechanism) seems to be favored against the e-transfer towards the e-accepting aromatic rings (geoconductor mechanism). As a consequence, these results suggest that external polarization enables the modulation of the e-accepting capability of carbon materials not only through the aromatic rings (geoconductor mechanism), but also by adjusting the ratio of HQ/Q groups (geobattery mechanism).

Nevertheless, the ca. 1000-times larger amount of CO-evolving groups (those potentially electroactive) on the biochar (Table 1) cannot explain why the removal efficiencies and rates of this material are "only" less than double those of the conductive carbon materials (Fig. 6). This effect could be reasonably explained by considering two facts. First, from this total amount of oxygen groups, only those accessible to electroactive bacteria and/or possible redox mediators may participate in e-transfer. Thus, XPS may provide a more realistic estimation of the (most accessible) surface oxygen functionalities. As it can be seen in Table S4, the proportion (%) of surface oxygen in the electroconductive biochar is "only" 2-10 times higher than in the other materials. Second, in a more amorphous and poorly conductive material like the biochar, the anodic polarization must be necessarily less efficient, so that a great part of its carbonaceous structure, including a large amount of potentially electroactive Q groups, may remain electrically disconnected and unaffected by polarization.

Finally, the proposed modulation of e-accepting Q groups and the electrical disconnection on poorly conductive biochar were confirmed when they were polarized at 0.6 V. Thus, compared to 0.4 V, at

0.6 V the conductive materials (coke and graphite) experienced a 20-30 % increment in COD removal efficiency, whereas the biochar only a 5 % (Fig. 6). If most of HQ groups on the biochar were oxidized at 0.4 V (as hypothesized), then a further increment of the electrode potential up to 0.6 V may lead to a lesser significant effect on the generation of Q groups and on the biodegradation. In addition, if the structure of this material is partly disconnected (as hypothesized), the e-accepting capability of aromatic rings (geoconductor mechanism) may be not so influenced by a higher potential than in the case of the high conductive materials. Consequently, a further increase in the electrode potential mainly increases the biodegradation capability of the most conductive carbon materials through the geoconductor mechanism. In other words, despite being globally less important than the geobattery phenomenon, the geoconductor mechanism becomes more significant with the electroconductivity of the carbon materials when they are polarized at higher potentials.

3.4 *Characterization of the bed materials after microbial colonization*

The bed materials were physico-chemically characterized also after being used as polarized working electrodes at 0.6 V to study the biofilm formation. The structural properties of the materials (XRD and Raman) were found to be practically unaffected, whereas their surface-related features changed after the wastewater treatment. The used gravel showed a surface morphology very similar to that before usage and individual bacteria were not discerned (Fig. S5). Nevertheless, the parallel decrease and slightly increase in the relative intensity of the Si(2p) and C(1s) XPS core-level signals, respectively (Table S4), suggested the formation of some biofilm.

On the contrary, more or less uniform biofilms were clearly observed on the different carbon materials (Figure 8). On the graphite, individual bacteria were identified only on some smooth regions (Fig. 8A-B), so that most of the wrinkled graphite sheets were covered by a roughened biofilm (Fig. 8C). As observed in this figure, this biofilm closely imitated the surface morphology of the pristine material, leaving the cracks and void regions unaffected. Accordingly, the Hg intrusion curves of this material and the derived textural parameters (Table 1) were practically identical before and after usage (Fig. 9A).

In the case of coke, the surface was totally covered by a biofilm (Fig. 8D), and some individual bacteria were difficult to discern (Fig. 8E). The biofilm was so dense (Fig. 8F) that it seemed to soften the crater-like holes of this material (compare Fig. 8D with Fig. 1C) and it even suffered from delamination in some zones (inset of Fig. 8F). Thus, unlike graphite, the biofilm slightly reduced the porosity of this material (Table 1), mainly affecting pores in the range of 20-10 μm (Fig. 9A).

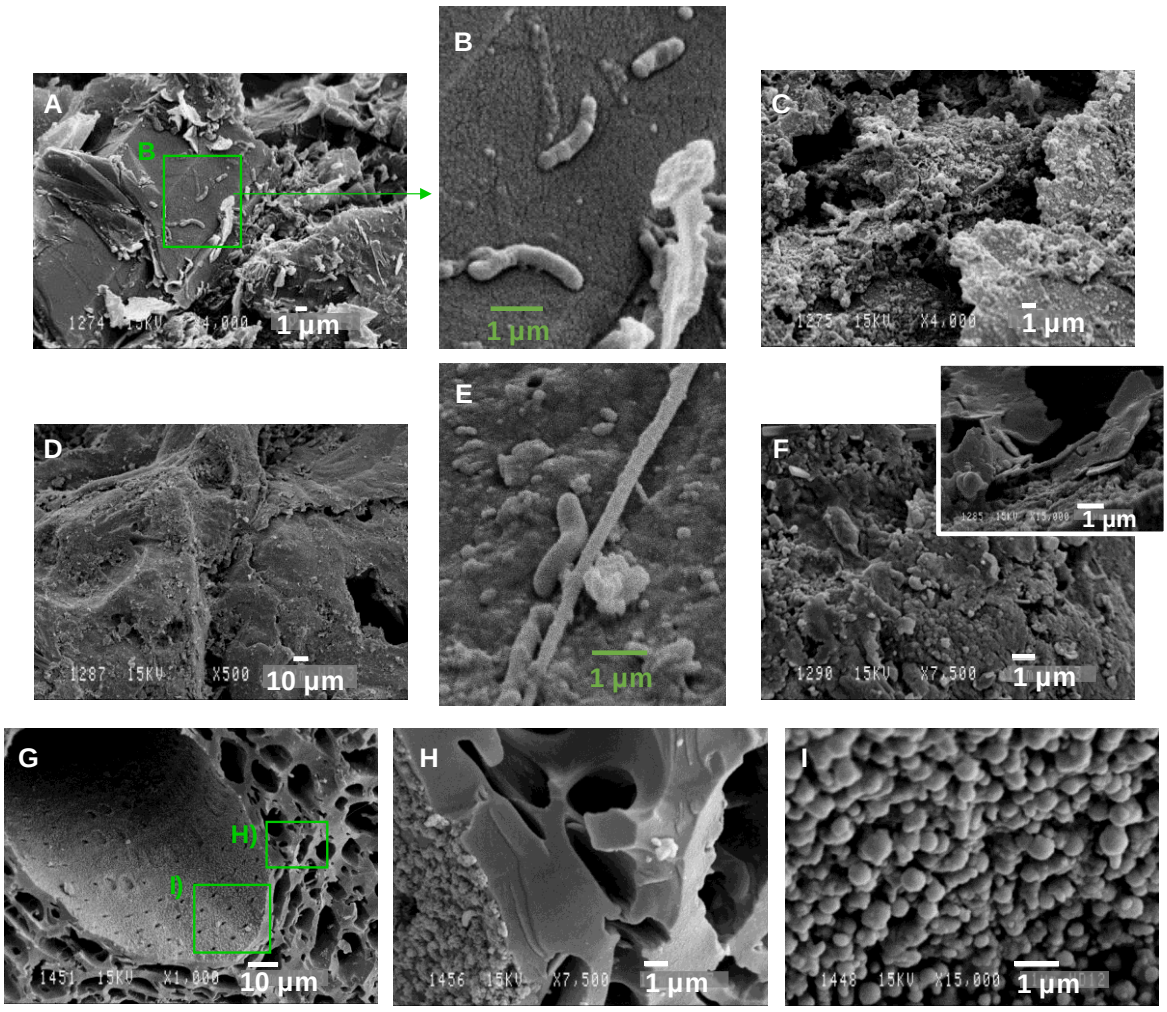

Figure 8. SEM micrographs of the carbonaceous bed materials after being used as polarized (0.6 V) electrogenic biofilters: (A-C) graphite; (D-F) coke; and (G-I) Quercus-derived biochar.

The biofilm formed on the biochar was quite different (Fig. 8G-I). The magnified images of the biochar (Fig. 8G) show that only the inner walls of the larger channels were colonized by microorganisms (Fig. 8H). This reflects certain selectivity of the bacteria for zones with, up to now, unknown particular features (dimensions, accessibility, etc.). Further magnification of these images reveals that the biofilm presents a spherical morphology (Fig. 8I). In addition, it can be observed that, despite forming a continuous film, they do not cover/block the pores of 1-2 µm in the inner walls of the large channels (see the Fig. 8G). Hence, the biofilm was found to affect mainly the pores of d < 300 nm (Fig. 9A and 9B), including the micropores (Vt) and ultramicropores (V_{CO2}), reducing the specific surface area of this material (Table 1). The comparison of surface chemical composition of the graphite and coke materials before and after usage as biofilters shows a relative decrease in surface C wt% probably related with the increase in O wt%, other heteroatoms (N, P, S) and metal impurities, mainly Fe (Table

S4). The same trend was observed for the biochar, but in this case the O wt% was practically unaffected.

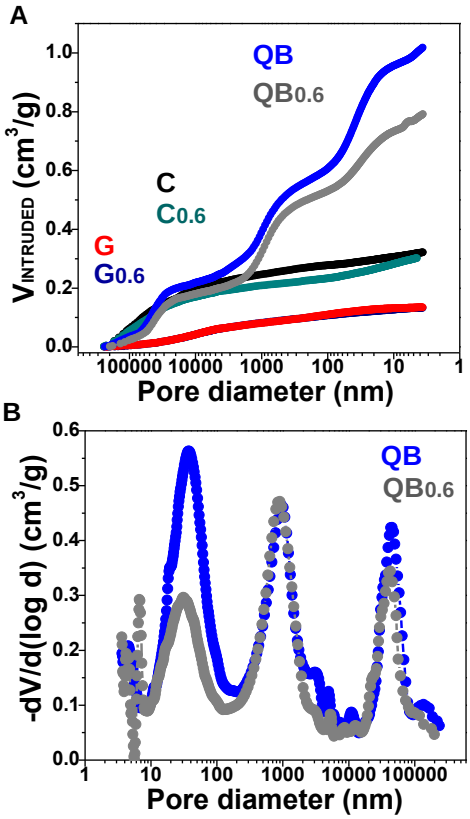

Figure 9. Hg Intrusion curves of the different carbon materials (A) and the pore size distribution of the Quercus-derived biochar, before and after being used as biofilters polarized at 0.6 V. G, graphite; C, coke; QB, Quercus electroconductive biochar.

It is well-known that these elements O, N, P, S and Fe are essential macro- and micro-nutrients for all organisms. Thus, although the original carbon materials contain some of these elements and although some adsorption from the contaminated water could occur, this more heterogeneous and complex surface of the used materials is attributed to the presence of the biofilm or its assimilated elements. In this sense, as a general trend, the biochar is the material showing the largest gain in Fe, N and S nutrients.

3.5 Electroconductive biochar: a sustainable material for constructing microbial electrochemical systems

The development of full-scale applications of METs for treating urban wastewater (ca. 150 L/habitant) will demand enormous amounts of carbon materials. In this context, the potential replacement of conductive carbon materials produced from fossil resources, like coke and graphite, by electroconductive biochars constitutes an attractive and sustainable strategy based on circular

economy. In addition, the high COD removal efficiencies of the biochar will lead to such a remarkable reduction of biofilter dimensions and/or area requirements to treat a given volume of water. Furthermore, considering that the electroconductive biochar shows the lowest density among the studied materials (Table 1), it can be easily deduced that a considerably lower mass of this material will be necessary for treating a given volume of wastewater. Finally, after its service life, the spent electroconductive biochar can be reutilized as soil amendment for giving a second life to this material.

Respect to cost, at present the production of biochar is in the same price range (400-600 euros/Tm) that cokes and graphites, which are obtained from large chemical industries or mining and subjected to market changes. However, the energy (thermal treatment) needed to prepare biochar is by far lower than that used to obtain mineral conductive materials. Consequently, electroconductive biochar production shows a lower CO_2 fingerprint, in addition to its "carbon negative" feature for taking more carbon out of the atmosphere than it puts back into it.

On the other hand, when polarized at 0.4 V and 0.6 V the biochar biodegradation rates lead to effluents with 4.2- and 6.6-fold lower residual COD values, respectively, than those produced by classical biofilter made of inert gravel. Hence, the results of this work allow to expand the up-to-now estimated potentiality of biofilter-based systems like the so-called METland® [5]. Even more important, our results may help to discern which are the best properties of a carbon material to optimize its performance for enhancing COD removal and/or for current production in METs. Among these properties, the presence of e-accepting quinone surface groups seems to be the essential to achieve higher biodegradations efficiencies, whereas the conductivity is probably the property determining the current-production. However, other typical properties of carbon materials, not considered until now, could also participate in the promotion of the biodegradation, so their study and understanding could lead to further optimization of METs.

In this sense, the present investigation demonstrates that the biochar exhibits various interesting features that cannot be found in the coke or graphite. For example, the high micropore volume and the presence of mesopores and small macropores ($d < 300$ nm) is exclusive of the biochar (Table 1). On the one hand, it is well known that the micropores are essential for the biochar (and other carbons) to storage electrons on the electrical double layer for energy storage [51]. The accumulation of a large number of electrons from bacteria, effectively compensated by the adsorption of ions on the micropores of the biochar, is likely to happen because of the low conductivity of this material. This could contribute to explain why all electrons released by bacteria are not "measured" as electrical current in our polarization assays (Fig. 6C-D). This agrees with the geobattery mechanism, in which

biochars can storage and reversibly exchange electrons [48]. On the other hand, it has been reported that small pores or other oxygen functionalities, like the carboxylic ones, could act as physical or chemical anchoring sites, respectively, to attach specific proteins or other functional parts of bacteria [52]. In addition, bigger pores may be necessary to host bacteria and biofilms. Consequently, apart from the proposed e-transfer mechanisms, the promotion of bioelectrochemical processes in METs could be also determined by the capability of the carbon materials to host bacteria, biofilms and/or electrons.

4. Conclusions

In this work, the performance of two fossil-derived and highly-conductive carbon materials (coke and graphite) for stimulating electroactive bacteria was compared with the one exhibited by biochar with lower electroconductivity but presenting a large volume of different pores and a rich variety of oxygen functionalities. Our studies revealed enhanced microbial EET and higher biodegradation rates when biochar was used as bed material for constructing biofilters under a wide range of operating conditions from non-polarized to polarized conditions. This optimal biodegradation performance has been mainly attributed to the electroactive oxygen functionalities on biochar, whereas the electroconductivity of the material and that of the biofilter bed determine the current production in these systems. Furthermore, we propose the modulation and promotion of its e-accepting capability by polarization, not only through the geoconductor mechanism, but also through the continuous regeneration of quinone-like functionalities (geobattery mechanism). The higher biodegradation efficiency showed by the electroconductive biochar (up to 6.6-fold higher than inert gravel) and the sustainability associated to its production (using renewable natural precursors at remarkably lower temperatures), will satisfy all circular economy criteria to expand the applicability of METs to biofilter-based systems like METland®.

Conflict of Interest

There are no conflicts to declare. All authors contributed equally to the work.

Acknowledgements

This investigation has received funding from the European Union's Horizon 2020 research and innovation programme under the grant agreement No. 642190 (Project "iMETLAND"; http://www.imetland.eu). Amanda Prado de Nicolás was funded by the "Formación de Personal Investigador (FPI)" PhD fellowship programme from the University of Alcalá. The authors thank the MINECO and FEDER (IJCI-2014-20012) for financial support.

References

[1] B. E. Logan, K. Rabaey, Conversion of Wastes into Bioelectricity and Chemicals by Using Microbial Electrochemical Technologies, *Science*, 2012, 337, 686-690.

[2] H. Wang, Z. J. Ren, A comprehensive review of microbial electrochemical systems as a platform technology, *Biotechnol. Adv.*, 2013, 31, 1796-1807.

[3] F. Caccavo, D. J. Lonergan, D. R. Lovley, M. Davis, Geobacter sulfurreducens sp. nov., a hydrogen- and acetate-oxidizing dissimilatory metal-reducing microorganism, *Microbiology*, 1994, 60, 3752-3759.

[4] A. M. Speers, G. Reguera, Electron Donors Supporting Growth and Electroactivity of Geobacter sulfurreducens Anode Biofilms, *Appl. Environ. Microbiol.*, 2012, 78, 437-444.

[5] A. Aguirre-Sierra, T. Bacchetti-De Gregoris, A. Berná, J. J. Salas, C. Aragón, A. Esteve-Núñez, Microbial electrochemical systems outperform fixed-bed biofilters in cleaning up urban wastewater, *Environ. Sci. Water Res. Technol.*, 2016, 2, 984-993.

[6] F. Aulenta, R. Verdini, M. Zeppilli, G. Zanaroli, F. Fava, S. Rossetti, M. Majone, Electrochemical stimulation of microbial cis-dichloroethene (cis-DCE) oxidation by an ethene-assimilating culture, *New Biotechnol.*, 2013, 30, 749-755.

[7] J. Rodrigo Quejigo, A. Domínguez-Garay, U. Dörfler, R. Schroll, A. Esteve-Núñez, Anodic shifting of the microbial community profile to enhance oxidative metabolism in soil, *Soil Biol. Biochem.*, 2018, 116, 131-138.

[8] A. Domínguez-Garay, J. R. Quejigo, U. Dörfler, R. Schroll, A. Esteve-Núñez, Bioelectroventing: an electrochemical-assisted bioremediation strategy for cleaning-up atrazine-polluted soils, *Microb. Biotechnol.*, 2018, 11, 50-62.

[9] R. Kadlec, S. Wallace, in Treatment Wetlands, 2nd Edition, CRC Press, Boca Raton, 2009.

[10] iMETland European H2020 project. http://imetland.eu/

[11] S. A. Patil, C. Hägerhäll, L. Gorton, Electron transfer mechanisms between microorganisms and electrodes in bioelectrochemical systems, *Bioanal. Rev.*, 2012, 4, 159-192.

[12] D. R. Lovley, Happy together: microbial communities that hook up to swap electrons, *ISME J.* 2017, 11, 327-336.

[13] X. Xie, C. Criddle, Y. Cui, Design and fabrication of bioelectrodes for microbial bioelectrochemical systems, *Energy Environ. Sci.*, 2015, 8, 3418-3441.

[14] M. Lu, Y. Qian, L. Huang, X. Xie, W. Huang, Improving the Performance of Microbial Fuel Cells, through Anode Manipulation, *ChemPlusChem*, 2015, 80, 1216-1225.

[15] J. M. Sonawane, A. Yadav, P. C. Ghosh, S. B. Adeloju, Recent advances in the development and utilization of modern anode materials for high performance microbial fuel cells, *Biosens. Bioelectron.*, 2017, 90, 558-576.

[16] Y. Hindatu, M. S. M. Annuar, A. M. Gumel, Mini-review: Anode modification for improved performance of microbial fuel cell, *Renew. Sust. Energ. Rev.*, 2017, 73, 236-248.

[17] S. Tejedor-Sanz, J. R. Quejigo, A. Berná, A. Esteve-Núñez, The planktonic relationship between fluid-like electrodes and bacteria: wiring in motion, *ChemSusChem*, 2017, 10, 693-700.

[18] T. Sun, B. D. Levin, J. J. Guzman, A. Enders, D. A. Muller, L. T. Angenent, J. Lehmann, Rapid electron transfer by the carbon matrix in natural pyrogenic carbon, *Nature Comm.*, 2017, 8, 14873.

[19] Y. Yuan, N. Bolan, A. Prévoteau, M. Vithanage, J. K. Biswas, Y. S. Ok, H. Wang, Applications of biochar in redox-mediated reactions, *Bioresour. Technol.*, 2017, 246, 271-281.

[20] K. Qian, A. Kumar, H. Zhang, D. Bellmer, R. Huhnke, Recent advances in utilization of biochar, *Renew. Sust. Energ. Rev.*, 2015, 42, 1055-1064.

[21] M.-M. Titirici, R. J. White, C. Falco, M. Sevilla, Black perspectives for a green future: hydrothermal carbons for environment protection and energy storage, *Energy Environ. Sci.*, 2012, 5, 6796-6822.

[22] J. Jiang, L. Zhang, X. Wang, N. Holm, K. Rajagopalan, F. Chen, S. Ma, Highly ordered macroporous woody biochar with ultra-high carbon content as supercapacitor electrodes, *Electrochim. Acta*, 2013, 113, 481-489.
[23] T. Huggins, H. Wang, J. Kearns, P. Jenkins, Z.J. Ren, Biochar as a Sustainable Electrode Material for Electricity Production in Microbial Fuel Cells, *Bioresour. Technol.*, 2014, 157, 114-119.
[24] P. Sennu, V. Aravindan, M. Ganesan, Y.-G. Lee, Y.-S. Lee, Biomass-Derived Electrode for Next Generation Lithium-Ion Capacitors, *ChemSusChem*, 2016, 9, 849-854.
[25] K. Kaetzl, M. Lübken, T. Gehring, M. Wichern, Efficient Low-Cost Anaerobic Treatment of Wastewater Using Biochar and Woodchip Filters, *Water*, 2018, 10, 818.
[26] H. P. Klug, L. E. Alexander in X-Ray Diffraction Procedures: For Polycrystalline and Amorphous Materials, 2nd Edition, Wiley-VCH, Weinheim, 1974.
[27] D. Lozano-Castelló, F. Suárez-García, D. Cazorla-Amorós, Á. Linares-Solano, in Carbons for Electrochemical Energy Storage and Conversion Systems, ed. F. Beguin, E. Frackowiak), CRC press, Boca Ratón, 2010, pp. 115-162.
[28] S. Lowell, J. A. Shields, M. A. Thomas, M. Thommes, in Characterization of Porous Solids and Powders: Surface Area, Pore Size and Density, Kluwer Academic Publishers, Dordrecht, 2004.
[29] APHA/AWWA/WEF, Standard Methods for the Examination of Water and Wastewater, 2012.
[30] A. R. Coutinho, J. D. Rocha, C. A. Luengo, Preparing and characterizing biocarbon electrodes, *Fuel Process. Technol.*, 2000, 67, 93-102.
[31] J. Rodríguez-Mirasol, T. Cordero, J.J. Rodríguez, High temperatura carbons from Kraft lignin, *Carbon*, 1996, 34, 43-52.
[32] Y. Wang, D. C. Alsmeyer, R. L. McCreery, Raman Spectroscopy of Carbon Materials: Structural Basis of Observed Spectra, *Chem. Mater.*, 1990, 2, 557-563.
[33] A. Cuesta, P. Dhamelincourt, J. Laureyns, A. Martínez-Alonso, J. M. D. Tascón, Raman microprobe studies on carbon materials, *Carbon*, 1994, 32, 1523-1532.
[34] N. Deprez, D. S. McLachlan, The analysis of the electrical conductivity of graphite conductivity of graphite powders during compaction, *J. Phys. D: Appl. Phys.* 1988, 21, 101-107.
[35] J. L. Figueiredo, M. F. R. Pereira, M. M. A. Freitas, J. J. M. Órfão, Modification of the surface chemistry of activated carbons, *Carbon*, 1999, 37, 1379-1389.
[36] H. Itoi, H. Nishihara, T. Ishii, K. Nueangnoraj, R. Berenguer, T. Kyotani, Large Pseudocapacitance in Quinone-Functionalized Zeolite-Templated Carbon, *Bull. Chem. Soc. Jpn.*, 2014, 87, 250-257.
[37] H. Richter, K. P. Nevin, H. Jia, D. A. Lowy, D. R. Lovley, L. M. Tender, Cyclic voltammetry of biofilms of wild type and mutant *Geobacter sulfurreducens* on fuel cell anodes indicates possible roles of OmcB, OmcZ, type IV pili, and protons in extracellular electron transfer, *Energy Environ. Sci.*, 2009, 2, 506-516.
[38] Council Directive 91/271/EEC of 21 May 1991 concerning urban waste-water treatment.
[39] F. Liu, A. E. Rotaru, P. M. Shrestha, N. S. Malvankar, K. P. Nevin, D. R. Lovley, Promoting direct interspecies electron transfer with activated carbon, *Energy Environ. Sci.*, 2012, 5, 8982–8989.
[40] J. García, D. P. L. Rousseau, J. Morató, E. Lesage, V. Matamoros, J. M. Bayona, Contaminant Removal Processes in Subsurface-Flow Constructed Wetlands: A Review, *Crit. Rev. Environ. Sci. Technol.*, 2010, 40, 561-661
[41] K. Rabaey, P. Clauwaert, P. Aelterman and W. Verstraete, *Environ. Sci. Technol.*, 2005, 39, 8077-8082.
[42] S. Chen, A. -E. Rotaru, P. M. Shrestha, N. S. Malvankar, F. Liu, W. Fan, K. P. Nevin, D. R. Lovley, Promoting Interspecies Electron Transfer with Biochar, *Sci. Rep.*, 2014, 4, 5019

[43] Z. Zhao, Y. Zhang, T. L. Woodard, K. P. Nevin, D. R. Lovley, Enhancing syntrophic metabolism in up-flow anaerobic sludge blanket reactors with conductive carbon materials, *Bioresour. Technol.*, 2015, 191, 140-145.
[44] Z. Zhao, Y. Zhang, D. E. Holmes, Y. Dang, T. L. Woodard, K. P. Nevin, D. R. Lovley, Potential enhancement of direct interspecies electron transfer for syntrophic metabolism of propionate and butyrate with biochar in up-flow anaerobic sludge blanket reactors, *Bioresour. Technol.*, 2016, 209, 148-156.
[45] D. R. Bond, D. R. Lovley, Electricity Production by *Geobacter sulfurreducens* Attached to Electrodes, *Microbiology*, 2003, 69, 1548-1555.
[46] W. Xu, J. J. Pignatello, W. A. Mitch, Role of Black Carbon Electrical Conductivity in Mediating Hexahydro-1,3,5-trinitro-1,3,5-triazine (RDX) Transformation on Carbon Surfaces by Sulfides, *Environ. Sci. Technol.*, 2013, 47, 7129-7136.
[47] M. A. Montes-Morán, D. Suárez, A. Menéndez, E. Fuente, On the nature of basic sites on carbon surfaces: An overview, *Carbon*, 2004, 42, 1219-1224.
[48] J. M. Saquing, Y. -H. Yu, P. C. Chiu, Wood-Derived Black Carbon (Biochar) as a Microbial Electron Donor and Acceptor, *Environ. Sci. Technol. Lett.*, 2016, 3, 62-66.
[49] R. Berenguer, R. Ruiz-Rosas, A. Gallardo, D. Cazorla-Amorós, E. Morallón, H. Nishihara, T. Kyotani, J. Rodríguez-Mirasol, T. Cordero, Enhanced electro-oxidation resistance of carbon electrodes induced by phosphorus surface groups, *Carbon*, 2015, 95, 681-689.
[50] R. Berenguer, F. J. García-Mateos, R. Ruiz-Rosas, D. Cazorla-Amorós, E. Morallón, J. Rodríguez-Mirasol, T. Cordero, Biomass-derived binderless fibrous carbon electrodes for ultrafast energy storage, *Green Chem.*, 2016, 18, 1506-1515.
[51] F. J. Chacón, M. L. Cayuela, A. Roig, M. A. Sánchez-Monedero, Understanding, measuring and tuning the electrochemical properties of biochar for environmental applications, *Rev. Environ. Sci. Biotechnol.*, 2017, 16, 695-715.
[52] M. Vijayaraj, R. Gadiou, K. Anselme, C. Ghimbeu, C. Vix-Guterl, H. Orikasa, T. Kyotani, S. Ittisanronnachai, The Influence of Surface Chemistry and Pore Size on the Adsorption of Proteins on Nanostructured Carbon Materials, *Adv. Funct. Mater.*, 2010, 20, 2489-2499.